UC Irvine
UC Irvine Previously Published Works

Title

Rapid Liquid Fuel Mixing for Lean-Burning Combustors: Low-Power Performance

Permalink

Journal

ISSN

Authors

Leong, MY
Smugeresky, CS
McDonell, VG
et al.

Publication Date

DOI

Copyright Information

Peer reviewed

M. Y. Leong[1]
Graduate Researcher

C. S. Smugeresky
Graduate Researcher

V. G. McDonell
Senior Research Scientist

G. S. Samuelsen[2]
Professor

UCI Combustion Laboratory
University of California
Irvine, CA 92697-3550

Rapid Liquid Fuel Mixing for Lean-Burning Combustors: Low-Power Performance

Designers of advanced gas turbine combustors are considering lean direct injection strategies to achieve low NO_x emission levels. In the present study, the performance of a multipoint radial airblast fuel injector Lean Burn injector (LBI) is explored for various conditions that target low-power gas turbine engine operation. Reacting tests were conducted in a model can combustor at 4 and 6.6 atm, and at a dome air preheat temperature of 533 K, using Jet-A as the liquid fuel. Emissions measurements were made at equivalence ratios between 0.37 and 0.65. The pressure drop across the airblast injector holes was maintained at 3 and 7–8 percent. The results indicate that the LBI performance for the conditions considered is not sufficiently predicted by existing emissions correlations. In addition, NO_x performance is impacted by atomizing air flows, suggesting that droplet size is critical even at the expense of penetration to the wall opposite the injector. The results provide a baseline from which to optimize the performance of the LBI for low-power operation. [DOI: 10.1115/1.1362318]

Introduction

The goal of the next generation of gas turbine combustors is to reduce NO_x emissions to meet regulatory levels that cannot be attained with present-day conventional combustors. In conventional gas turbine combustors, thermal NO_x is one of the major contributors to overall NO_x production. Thus, the reduction of NO_x is mainly accomplished by lowering the reaction temperature, which itself can be achieved by operating the combustor under fuel-lean conditions. The attainment of a lower level of NO_x production by these lean-burning, advanced gas turbine combustors primarily depends on the preparation of the fuel-air mixture by fuel injectors. NO_x production increases with fuel-air unmixedness in both spatial (Lyons [1]) and temporal domains (Fric [2]). Although the mixture may be overall lean, a wide distribution of local equivalence ratios that bracket the stoichiometric condition will encourage thermal NO_x production. These lean-burning, low-NO_x combustion concepts, though, are not without disadvantages. For example, operating near the lean flammability limit runs the risk of combustor blow out or combustor instability. In addition, the levels of carbon monoxide (CO), unburned hydrocarbons (UHC), and air toxics (e.g., aldehydes) may increase to unacceptable levels. Low-NO_x combustion methods that burn fuel-lean must overcome these challenges in order to become a viable technology.

One low-NO_x lean combustion concept—the lean-premixed-prevaporized (LPP) combustor—involves the introduction of a uniformly lean mixture of fuel vapor and air into the dome region of a combustor. Low NO_x levels can be achieved by burning the fuel in its vapor phase rather than as droplets (Lefebvre [3]). The low-NO_x potential of LPP combustion has led to studies characterizing the effect of mixing on combustion instability and emissions (e.g., Shih et al. [4]; Dutta et al. [5]). However, the premixed state of the fuel and air makes LPP combustion prone to autoignition and flashback. In addition, the stability limits of the LPP combustor tend to fall in a narrow range, and ignition of the mixture may be difficult.

Another fuel preparation concept for lean-burning combustors is lean direct injection (LDI), in which fuel is injected immediately upstream of the reaction zone, thereby reducing the potential for autoignition and allowing for smaller overall combustion system dimensions. The low-NO_x potential of the LDI has mainly been demonstrated for gaseous fuel injection (Tacina, [6]), but the challenges of atomizing and vaporizing liquid fuel sufficiently for low-NO_x, LDI combustion have been met with the lean burn injector (LBI). The LBI nozzle prepares a vaporized fuel-air mixture (as in the LPP concept) for combustion in the confines of a contracting mixing section. Developed by Shaffar, Sowa, and Samuelsen [7], the LBI assembly consists of a fuel tube centerbody, swirler, and venturi mixing section that is also referred to as a ''quarl'' (Fig. 1). Rapid mixing of liquid fuel and air is achieved by injecting spray jets of fuel radially from the center body, into a swirling crossflow of air. The sprays are formed by airblast atomization, which allows for higher fuel turndown ratios compared with pressure-swirl atomizers. The fuel sprays mix with the swirling air in the contracting venturi section. The fuel-air mixture is subsequently ejected out of the venturi section and into the primary dome of the combustor. The swirling component in the fuel-air mixture induces the recirculation zone that anchors the combustion process. As noted by Shaffar and Samuelsen [8], combustion stabilizes downstream of the venturi throat, which also helps to prevent flashback. The quarl section, serving as both a fuel-air premixing section and as a flame arrestor, is the main novel feature of the LBI injector assembly.

The LBI concept can be applied to aeroengine and industrial engine, and to conventional as well as to the next generation of low-NO_x combustors. However, the thrust of the current development involves investigating the performance of the LBI for a low-NO_x aeroengine application. Shaffar and Samuelsen [8] demonstrated low NO_x performance with NO_x EI less than 9 for a condition of 5 atm. 700 K preheat, between $\phi = 0.45–0.70$. To prove the potential utility and versatility of the injector across the entire aeroengine duty cycle, a baseline survey of LBI performance must be established. The objective of the present study is to evaluate the robustness of the LBI design for low-NO_x combustion, primarily at low-power conditions where low preheat temperatures and pressures may not fully atomize and vaporize drops before the mixture exits the quarl mixing section. The effect of spray atomi-

---
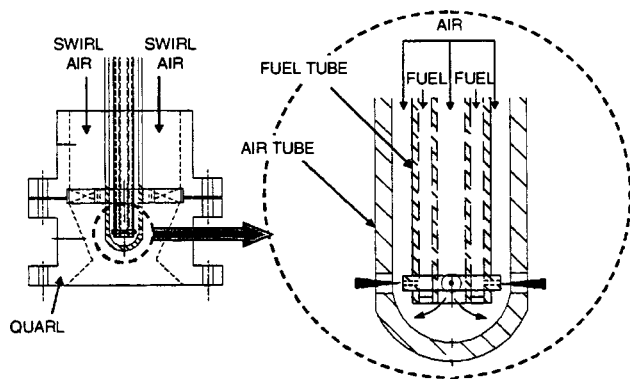
Fig. 1   LBI injector, swirler, and quarl assembly

Fig. 2   LBI injector, combustor in elevated pressure facility

zation on combustion performance is evaluated by varying the atomizing air supply to the injector. Emissions measurements are primarily used to assess combustion performance in terms of low-NO_x and high combustion efficiency, and are compared with the predictions of existing correlations.

Experiment

LBI Injector.   The LBI assembly (Fig. 1) consists of an eight-port injector, a production cast swirler with a swirl number of 2.2, and a quarl. The LBI injector used in the combustion tests employs the same design used by Shaffar and Samuelsen [8]. The injection lance is comprised of a fuel tube and an outer air tube. The fuel tube itself is comprised of two concentric tubes with the tip of the annular region welded shut so that fuel can only exit through eight holes that are 0.66 mm diameters each, drilled radially through the tube and an outer ring welded on to the outside of the tube. The atomizing air (9–15 percent of the mass flow of dome air) flows through the center of the fuel tube as well as through the annulus formed by the outer fuel tube and the inner air tube. The airblast-atomized spray emerges from holes drilled in the outer air tube. The total effective area of all eight air orifices is 36.1 mm^2. The injection point occurs 19.1 mm downstream from the swirler vanes, and 18.5 mm upstream of the quarl contraction.

The main difference between the present injector and the injector used by Shaffar and Samuelsen lies in the dimension of the fuel hole diameter, which was enlarged to preclude potential coking issues for the range of operating conditions considered. The enlargement does not impact the basic behavior of the spray as indicated by the study of Lorenzetto and Lefebvre [9], which found that initial fuel stream diameter has little effect on the spray behavior of low viscosity liquids atomized by plain-jet airblast atomizers.

Elevated Pressure Facility for Combustion Tests.   The LBI combustor tests are conducted in a pressure facility designed primarily for reacting experiments (Fig. 2). The LBI injector is installed in a model 80 mm ID can combustor assembly that is downward fired. The combustor is bolted to the bottom flange of the pressure vessel. The cylindrical vessel has an inside diameter of 0.30 m and a height of 0.86 m. Four 152 mm diameter ports along the circumference of the vessel provide optical access as well as an opening for the insertion of an emissions probe. Smaller ports are also available in the vessel wall for thermocouples and pressure taps. The top of the vessel is a blind flange through which the LBI injector tube passes. The injection tube is secured to the vessel after it is inserted into the combustor assembly. The products of this down-fired combustion rig pass through a water quench section before exhausting. Vessel pressure is regulated by a control valve downstream of the water quench system.

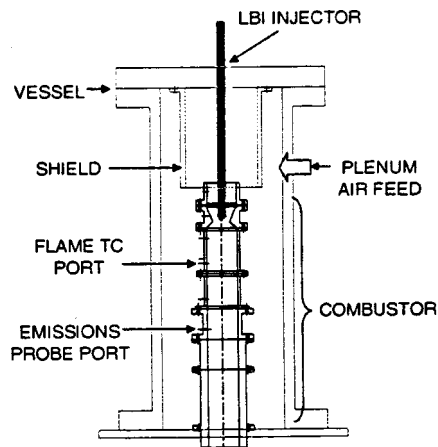The facility utilizes two separately metered air circuits—a high flow line to feed the plenum of the pressure vessel, and a low flow line to supply the atomizing air. The air flows are controlled by a system of thermal mass flow meters and electropneumatic control valves. Both air circuits can be heated by electric circulation heaters. However, in this experiment, the injector atomizing air was not heated in order to establish a baseline condition for future tests involving the effect of airblast air temperature on fuel-air mixing and combustion performance.

Measurements.   Emissions samples were obtained 271 mm downstream of the quarl throat. At this point, the calculated bulk residence time of the combustion products is 8 msec. The emissions sampling system utilized the pressure differential between the experiment and the exhaust at atmospheric pressure to drive the sample through the probe. A multiport water-cooled probe 12.7 mm in diameter was designed to yield area-weighted emissions across the combustor can.

The sampling procedure involved individual, independent measurement of emissions at each port. The gas sample was sent through an ice water bath to condense the water in preparation for the analyzers, which measure dry gas sample concentrations. The residence time of the sample from the probe to the ice bath was approximately 1 sec. Any condensate forming in this section of the line was filtered at the water dropout station immediately downstream of the ice water bath. The possibility of NO_2 dissolving in the condensate existed, but the loss was presumed minimal because of the short residence time that the sample gases were in contact with the water.

With the sample gas venting to an exhaust hood, a pump in a sampling unit (Horiba ES-510) drew a slip stream of gas. The sample was then split and sent to two units for analysis. The total unburned hydrocarbon concentrations were measured by a flame ionization analyzer (Horiba FIA-510) while CO, CO_2, O_2, and NO_x were measured by a portable gas analyzer (Horiba PG-250). The portable gas analyzer employs non-dispersive infrared (NDIR) methods to measure CO and CO_2, a galvanic cell to measure O_2, and chemiluminescence to measure NO_x. The uncertainty associated with the analyzers is within 1 percent of the full scale reading.

The analog signals from the emissions analyzers were collected through an 8-channel, 16-bit analog input board (National Instruments FP-AI-110), which was connected to a computer through an RS-485 network interface board (National Instruments FP-1001). A routine written in the software program that accompanied the boards (LABVIEW 5.0, National Instruments) recorded and processed the signals. The signals from the analyzers were sampled at a rate of 2 Hz, for a duration of 50 sec. The mean emissions data exhibited a stationary temporal distribution. Temporal signal fluctuations only contributed up to 1 percent of the overall uncertainty.

Table 1 Operating conditions for the LBI low-power tests

Case name	P_3 (kPa)	m_{air} (kg/sec)	$m_{airblast}$ (kg/sec)	$\Delta R_{airblast}$ (%)
4 atm/8 DP	412	0.15	0.021	8
4 atm/3 DP	412	0.15	0.014	3
6.6 atm/7 DP	670	0.24	0.035	7
6.6 atm/3 DP	670	0.24	0.023	3

Table 2 Lean blow-out levels for the various tests

Condition	LBO
4 atm/8 DP	0.42
4 atm/3 DP	0.41
6.6 atm/7 DP	0.43
6.6 atm/3 DP	0.36

The computerized data acquisition system also sampled thermocouple readings at the same rate. Type-K chromel-alumel thermocouples were used to measure the temperature of the preheated dome air prior to its passage through the swirler, as well as the temperatures of the nozzle air, fuel, and combustor skin. A type-B platinum-rhodium thermocouple monitored the bulk reaction temperature 106 mm downstream from the quarl throat. The shielded 1.59 mm OD type-B thermocouple was also sheathed with a 3.18 mm OD alumina ceramic cover to protect the thermocouple from the harsh turbulent and reacting environment. The reported temperatures were corrected for radiation heat loss. The uncertainty associated with the temperature measurements were as high as 2 percent of the corrected values.

Test Matrix. To assess the utility of the LBI injector in aeroengine applications, the injector is tested at practical conditions. The flow rates in these tests are comparable to the low-power regime of ground idle and subsonic cruise conditions. The four cases and their main operating parameters are listed in Table 1. Two ambient pressure cases were tested: 412 kPa (4 atm) and 670 kPa (6.6 atm). The overall mass flow of air m_{air} through the combustor, which is the sum of the swirl and atomizing air mass flow rates, was determined by the combustor pressure drop, which was maintained at 4 percent. For each ambient pressure condition, the atomizing air flow was set at two pressure drops that bracketed the typical range of air pressure drops available in aeroengine combustors (4–7 percent, according to Lefebvre [3]). The airblast velocity remained constant at a given pressure drop condition, for different ambient pressures.

While the overall air mass flow rate was kept constant, the fuel-air equivalence ratio was changed by varying the fuel flow rate of Jet-A (Unocal). Measurements were begun at an equivalence ratio between 0.55 and 0.65. Emissions concentrations were measured after lowering the equivalence ratio in increments of 0.05. After attaining the desired condition, the system was given 5–10 min to thermally stabilize before measurements were obtained. For all of the tests, a fuel air ϕ as low as 0.45 was reached. After attaining the $\phi=0.45$ level, the equivalence ratio was decreased further by increments of 0.01 until LBO occurred. In three of the cases. LBO occurred between 0.41 and 0.43 (see Table 2). At the 6.6 atm/3 percent dp condition, LBO occurred at $\phi=0.36$.

Results and Discussion

Combustion Product Uniformity. A radial profile of emissions samples was obtained for each case to yield an area-weighted average. The area-weighted average CO_2 and O_2 concentrations were compared with their respective equilibrium values calculated at corresponding equivalence ratio conditions. The emissions measured for the 4 atm cases agreed well to within 2 percent of predicted values, whereas the emissions for the 6.6 atm cases varied up to 15 percent of predicted values.

Radial profiles for the measured species concentration samples are presented in Fig. 3 for the 4 atm/8 percent dp case. The uniform radial profiles of CO_2 and O_2 seen in this case at the different equivalence ratios were also typical of the other three cases.

The CO, UHC, and NO_x radial concentration profiles in this 4 atm/8 percent dp case were also uniform at equivalence ratios ranging from 0.50 to 0.65. The magnitude of the profiles decreased as ϕ decreased from 0.65 to 0.50. At $\phi=0.45$, the leanest

equivalence ratio that was measured in this case, the radial profile was uniform for NO_x, but nonuniform for the CO and UHC emissions.

Figure 4 presents a condensed depiction of the radial profile uniformity, as represented by the standard deviation of the concentrations measured at each condition. Only the profiles for CO_2, NO_x, and CO are shown for clarity, since the trends for O_2 mirrored those for CO_2, and since the trends for UHC closely followed those for CO.

The standard deviations for each test case are plotted with respect to equivalence ratio. Lower standard deviation values correspond to a more uniform radial concentration profile. The shape of the curve indicates how the degree of uniformity changes with respect to equivalence ratio.

The standard deviation values for the 4 atm/8 percent dp case summarize the observations made in Fig. 3 for the case. For example, uniform CO_2 profiles at each equivalence ratio, observed in Fig. 3, are represented by the low standard deviation values in Fig. 4. The small degree of variation in the curve for CO_2 reflects the uniformity in profiles at the different ϕ. The nonuniform CO profile obtained at $\phi=0.45$ in this case (see Fig. 3) is reflected by a high standard deviation value at that equivalence ratio (see Fig. 4).

In all of the cases tested, the radial profile of concentrations became more uniform as leaner equivalence ratios were attained. Two exceptions to this point are found in the CO profile measurement. As discussed earlier, the 4 atm/8 percent dp case produced a highly nonuniform CO profile at the $\phi=0.45$ condition. Likewise, the 6.6 atm/3 percent dp condition produced a similar result near the lean blow-out limit, at $\phi=0.37$. Similar high CO standard deviation values in the 4 atm/3 percent dp and 6.6 atm/7 percent dp cases would probably have been achieved if emissions measurements had been made near the LBO limit.

Bulk reaction temperatures were measured nearly halfway between the quarl throat and the emissions probe, where the thermocouple protruded 25 mm into the combusting flow. The temperatures shown in Fig. 5 represent time-averaged values across the sampling duration of emissions at the particular equivalence ratio condition.

At a given equivalence ratio, the bulk reaction temperature should be the same. Figure 5, however, shows some deviation in the measured temperatures, particularly for the equivalence ratios from 0.45 to 0.55. The 4 atm/8 percent dp case produced temperatures that were significantly higher than those from the other 3 cases, which amongst themselves registered temperatures within an experimental uncertainty of ±20 K. The differences in reaction temperature between the cases show that, though uniform flow may have been achieved at the plane of the emissions probe, uniform flow may not have yet been attained at the plane of the thermocouple.

Combustion Performance. Two parameters used to assess combustion performance are the combustion efficiency and the production of pollutant emissions. The gas turbine combustor should operate at a high efficiency while forming minimal levels of pollutants.

The combustion efficiency η, calculated from the CO and UHC emissions, indicates the degree to which complete combustion products is attained. As seen in Fig. 6, the LBI injector combustion efficiency is above 99.90 percent for every condition except
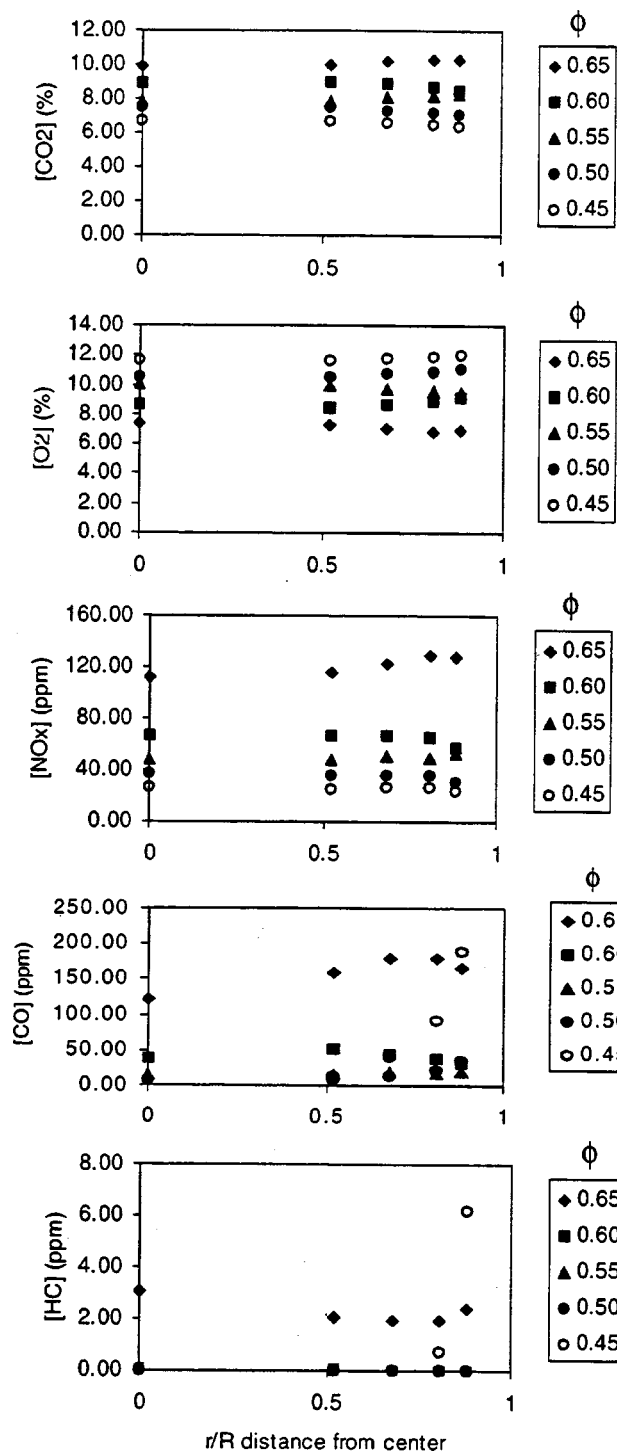
Fig. 3 Radial emissions profile for the 4 atm/8 percent DP case

Fig. 4 Standard deviation values indicating radial profile uniformity at different equivalence ratios

Fig. 5 Bulk temperature measured 106 mm downstream of quarl throat

most 1800 K, the steep exponential NO_x formation rate associated with the thermal mechanism is avoided (Samuelsen [10]; Lefebvre [3]).

For a given airblast pressure drop, a direct comparison can also be made between different ambient pressure conditions because the ALRs were also kept constant at each equivalence ratio. In cases with similar airblast pressure drops, an increase in ambient pressure generally led to an increase in the NO_x EI.

Existing emissions correlations were compared with measured NO_x and CO concentrations to determine their applicability to the LBI combustion process. NO_x and CO correlations developed by Lefebvre [11] and by Rizk and Mongia [12] were applied. Lefebvre's correlations are primarily used for conventional spray combustors, but can be applied to LPP combustion with a suitable temperature variable substitution. The correlations of Rizk and Mongia [12] include the effects of spray evaporation and mixing on combustion emissions production.

When applied to the LBI data, the ''spray version'' of the Lefebvre [11] correlation and the Rizk and Mongia [12] correlations produced NO_x and CO trends that were inversely proportional to

the 6.6 atm/3 percent dp case where emissions obtained at $\phi=0.37$ near the LBO limit led to a 99.57 percent efficiency (not shown in the figure). In general, at each pressure condition, higher efficiencies are obtained for the 7–8 percent airblast pressure drop condition than for the corresponding 3 percent pressure drop case.

Pollutant emissions are often represented by emission indices (EI), which cast the volumetric measurements of the emissions onto a mass basis. Figure 7 shows the NO_x EI across the range of equivalence ratios tested in each case. The NO_x EI measured are all below 5, which can be attributed to the low reaction temperatures seen in Fig. 5. With overall reaction temperatures reaching at
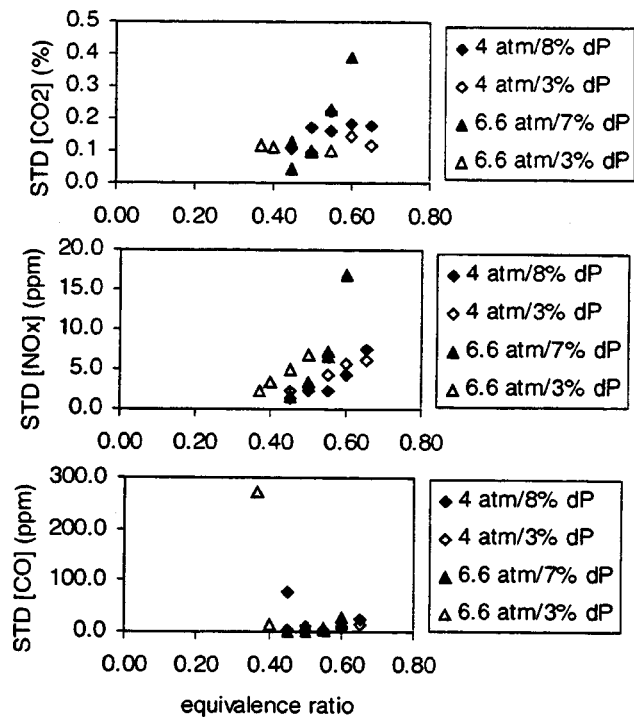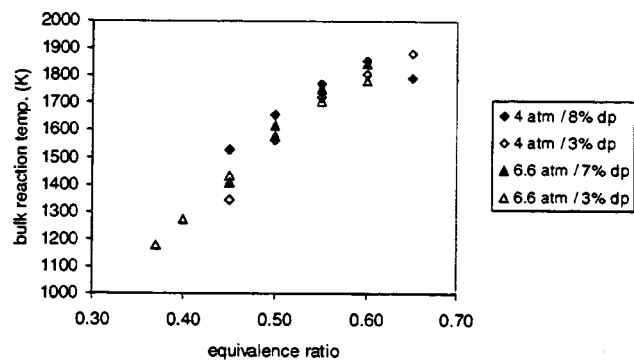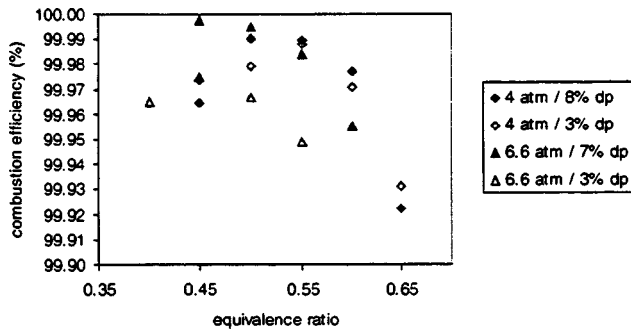
Fig. 6 LBI combustion efficiencies at the various operating conditions
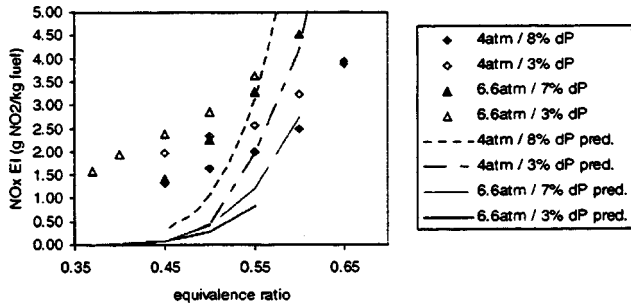
Fig. 7 Spatially averaged NO$_x$ emission indices overlaid with LPP predictions from Lefebvre [10]

Fig. 8 Droplet D_{32} as predicted by the Lorenzetto and Lefebvre correlation [9]

the measured values. The ''LPP version'' of the Lefebvre correlation predicted NO$_x$ EI and CO EI trends that were similar to the measured data, but were also unsatisfactory in their accuracy.

The NO$_x$ curves predicted by the ''LPP version'' of the Lefebvre correlation, shown overlaid on the NO$_x$ EI plot in Fig. 7, illustrate the lack of fit to the data. As seen in Fig. 7, the curves follow the decreasing NO$_x$ with decreasing ϕ data trend. However, the NO$_x$ EI curve for the 7–8 percent airblast dp cases are higher than the corresponding 3 percent cases for each pressure condition. For the constant overall air flow rates at the 4 and 6.6 atm cases, the predicted curves should coincide for these pressure conditions. In addition, the 4 atm cases are predicted to produce higher NO$_x$ EI than the 6.6 atm cases. The main parameters that vary in the Lefebvre correlation are pressure and the primary zone temperature, and since the measured reaction temperatures, depicted in Fig. 5, were already shown to deviate at each ϕ condition, the NO$_x$ EI predictions were also similarly affected. In any case, this insufficient fit by the LPP-based Lefebvre correlation and by the spray combustor model of Rizk and Mongia points toward the need to measure and model the fuel-air mixture characteristics in and immediately downstream of the quarl so that the model can accommodate the mixing features of the LBI injector.

Spray Atomization and Penetration. To explain the combustion performance in relation to fuel atomization and mixing, spray droplet size and penetration correlations were utilized. The droplet size of interest in combusting flows is D_{32}, which represents the ratio of the total volume to the total surface area of the spray droplets. The D_{32} values of the sprays produced in this experiment were calculated using the Lorenzetto and Lefebvre [9] correlation for plain-jet airblast atomizers, which according to Shaffar and Samuelsen [8] satisfactorily predicted the droplet size of sprays from the LBI injector.

Figure 8 shows the predicted droplet sizes for the conditions tested, as well as for the LBO limits. The similar D_{32} values obtained at the same airblast pressure drop conditions reflect the similar airblast air to liquid mass flow ratios (ALR) used in these cases.
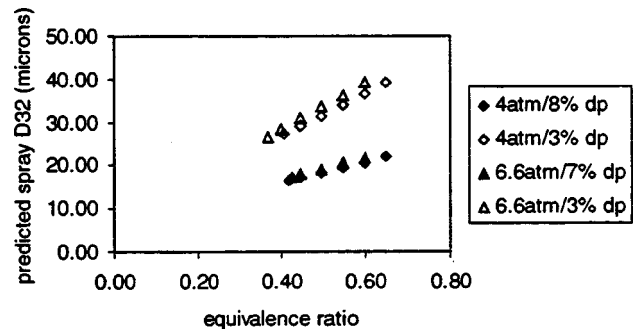
As the fuel flow is lowered to decrease ϕ, the ALR increases. Higher airblast pressure drops, which increase the relative velocities between the atomizing air and fuel stream also lead to higher ALRs. In airblast sprays higher ALRs result in smaller D_{32} (Lefebvre [13]). Smaller droplets vaporize faster than larger droplets, resulting in faster fuel vapor mixing with air. Thus, at higher airblast pressure drops, one expects lower NO$_x$ emissions resulting from smaller droplet sizes, as the data in Fig. 7 depict. Risk and Lefebvre [14] also observed this relationship between decreasing droplet size and lower NO$_x$ emissions in their study.

In relation to the uniformity of the emission fields, decreasing D_{32} values corresponded to increasingly uniform emissions fields at lower equivalence ratios up until the point when LBO is reached (see Fig. 4). The higher combustion efficiencies obtained with increased airblast pressure drop also correlated to the smaller droplet D_{32} values that occur here at the lower ϕ (see Fig. 6).

Despite the small droplet D_{32} produced by airblast atomization, the conditions of the tests did not induce full vaporization of the spray by the quarl exit plane. The droplet evaporation times calculated for the given operating conditions and droplet sizes were at least four times greater than the calculated residence time of the spray from the point of injection to the quarl exit (0.75 msec), suggesting that droplets persisted in the dome region.

The penetration of the spray into the swirling dome air can be predicted by a modified correlation describing the maximal spray surface trajectory into the crossflow. Leong et al. [15] derived a correlation from images captured, in an experiment modeled after the LBI hardware, of a single spray jet injected into a uniform crossflow. Although the trajectory analysis neither accounts for the highly nonuniform velocity profile in the quarl contraction nor for droplet vaporization, the correlation can give a general estimate of spray penetration into the quarl.

In the spray correlation of Leong et al. [15], images were obtained at ambient pressures of 1, 3, and 5 atm, at different airblast pressure drops. The trajectory of maximum penetration was described by an equation that incorporated a jet-to-crossflow momentum-flux ratio. For a single phase jet, the momentum-flux ratio is clearly defined, but for a two-phase flow, such as the airblast spray jet, the momentum-flux ratio must incorporate the momentum of both liquid and airblast air streams. The following definition was developed in the 1998 work to describe the two-phase momentum-flux ratio q_2:

$$q_2 = \{[(\rho V^2 A)_{\text{fuel}} + (\rho V^2 A)_{\text{airblast}}]/A_{\text{jet}}\}/(\rho V^2)_{\text{crossflow}}, \quad (1)$$

where A_{airblast} is the annular area corresponding to A_{jet} minus A_{fuel}, and $V_{\text{crossflow}}$ corresponds to the bulk crossflow velocity at the point of injection. The derived correlation described the upper surface trajectory well at the 3 atm case, but underpredicted the spray trajectories at the 1 atm condition, and overpredicted the trajectories at the 5 atm condition.
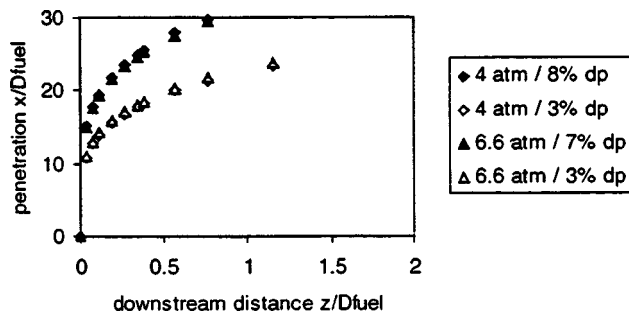
Fig. 9 Upper spray penetration predicted by modified correlation of Leong et al. [15]

One reason for the insufficient fit lies in the lack of a term to account for the atomization quality of the spray. Adding the factor (D_{32}/D_{fuel}) to the curve fit of Leong et al. [15] to account for the droplet size greatly improved the correlation. A least squares analysis performed with the additional factor resulted in the following curve fit which describes the upper surface penetration x/D_{fuel}:

$$x/D_{fuel}=(A1)*q_2^{A2}*(z/D_{fuel})^{A3}*(D_{32}/D_{fuel})^{A4}, \qquad (2)$$

where z/D_{fuel} represents the downstream distance, and constants $A1=13.8$, $A2=0.67$, $A3=0.22$, and $A4=0.39$.

The q_2 values ranged between 28–29 for the 7–8 percent airblast pressure drop cases, and between 12–13 for the 3 percent dp cases. Varying the liquid fuel flow to achieve different equivalence ratios does not significantly impact the value of q_2. The result of applying the modified correlations of Leong et al. using the q_2 values for the present test conditions is shown in Fig. 9.

At the point of spray injection, the distance between the LBI injection tube to the quarl wall is 16 mm. Furthermore, the continued contraction of the quarl section narrows the gap between the injector and the quarl wall. Thus, to avoid wall impingement, the spray trajectory should, at a minimum, penetrate no farther than $x/D_{fuel}=27$. The plot in Fig. 9 shows that all of the cases produce sprays that can impinge on the quarl wall. The 3 percent airblast dp sprays reveal relatively more bending into the cross flow with a reduced possibility of quarl impingement.

The calculated time that it would take for the spray to travel the distance from the injection point to the quarl wall, based on the bulk relative velocity of the droplets, varies from 0.14 to 0.23 msec, which is an order of magnitude less than the estimated total vaporization time of the droplets. This suggests that wall impingement most likely occurs, with the droplets either flash vaporizing upon collision with the wall, or possibly reatomizing after the impacted fluid shears off the lip of the quarl throat.

Summary and Conclusions

The LBI injector, which combines the direct injection principle with a short mixing section, was tested under various ambient pressures and with different atomizing air flows to assess its performance at low-power engine conditions. Radial profiles of species concentrations were generally uniform, with increasing spatial uniformity occurring as leaner equivalence ratios were attained, up until a point near lean blow out.

The atomization quality of the spray is primarily affected by the pressure drop of the atomizing air as well as the atomizing air to liquid mass flow ratio (ALR). A high airblast pressure drop (7–8 percent) and a high ALR (achieved in this experiment at leaner equivalence ratios), correspond to a decrease in D_{32}. This in turn produces a lower NO_x EI and higher combustion efficiencies. The improvement continues up to an equivalence ratio in the near

vicinity of lean blow out. Despite achieving finer droplets, it is probable that the spray droplets persist in the flow at the relatively low air preheat temperature associated with low power operation.

We conclude the following.

1 The LBI is an attractive strategy for the introduction of fuel and the promotion of rapid mixing. At low power conditions, attention must be directed to the identification of design and operation parameters that minimize (and preclude) the penetration of liquid fuel to the quarl wall.

2 The crossflow injection of evaporating droplets presents novel challenges for existing penetration and emissions correlations. The effects of pressure, air preheat, initial spray characteristics (e.g., size distribution, component of swirl), atomizing air properties, and fuel properties), and secondary atomization have particular significance in crossflow configurations.

Nomenclature

ALR = airblast air to liquid mass flow ratio
D_{32} = total droplet volume to total droplet surface area ratio
EI = emission index, (g emission)/(kg fuel)
LBO = equivalence ratio at which lean blow-out occurs
q_2 = two-phase jet to crossflow momentum-flux ratio
ϕ = fuel-air equivalence ratio

References

[1] Lyons, V. J., 1981, ''Fuel/Air Nonuniformity—Effect on Nitric Oxide Emissions,'' AIAA J., **20**, pp. 660–665.
[2] Fric, T. F., 1993, ''Effects of Fuel-Air Unmixedness on NO_x Emissions,'' J. Propul. Power , **9**, pp. 708–713.
[3] Lefebvre, A. H., 1999, *Gas Turbine Combustion*, 2nd ed., Taylor and Francis, Philadelphia, PA.
[4] Shih, W. P., Lee, J. G., and Santavicca, D. A., 1996, ''Stability and Emissions Characteristics of a Lean Premixed Gas Turbine Combustor,'' *Twenty-Sixth Symposium (International) on Combustion*, pp. 2771–2778.
[5] Dutta, P., Gore, J. P., and Sojka, P. E., 1997, ''Emissions Characteristics of Liquid-Fueled Lean Premixed Flames in a Tubular Premixer-Combustor,'' J. Eng. Gas Turbines Power, , **119**, pp. 585–590.
[6] Tacina, R. R., 1990, ''Low-NO_x Potential of Gas Turbine Engines,'' AIAA Paper 90–0550.
[7] Shaffar, S. W., Sowa, W. A., and Samuelsen, G. S., 1995, ''Lean Burn Injector for Gas Turbine Combustor,'' U.S. Patent No. 5,477,685, 26 December.
[8] Shaffar, S. W., and Samuelsen, G. S., 1998, ''A Liquid Fueled, Lean Burn, Gas Turbine Combustor Injector,'' Combust. Sci. Technol. **139**, pp. 41–57.
[9] Lorenzetto, G. E., and Lefebvre, A. H., 1977, ''Measurements of Drop Size on a Plain Jet Airblast Atomizer,'' AIAA J., **15**, pp. 1006–1010.
[10] Samuelsen, G. S., 1975, ''The Combustion Aspects of Air Pollution,'' in *Advances in Environmental Science and Technology*, John Wiley & Sons, New York, Vol. 5. pp. 219–322.
[11] Lefebvre, A. H., 1984, ''Fuel Effects on Gas Turbine Combustion—Liner Temperature, Pattern Factor, and Pollutant Emissions,'' J. Aircr., **21**, No. 11, pp. 887–898.
[12] Rizk, N. K., and Mongia, H. C., 1993, ''Semi-analytical Correlations for NO_x , CO, and UHC Emissions,'' J. Eng. Gas Turbines Power, **115**, pp. 612–619.
[13] Lefebvre, A. H., 1992, ''Twin Fluid Atomization: Factors Including Mean Drop Size,'' Atomization Sprays **2**, pp. 101–119.
[14] Rink, K. K., and Lefebvre, A. H., 1989, ''The Influence of Fuel Composition and Spray Characteristics on Nitric Oxide Formation,'' Combust. Sci. Technol. **68**, pp. 1–14.
[15] Leong, M. Y., McDonell, V. G., and Samuelsen, G. S., 1998, ''Effect of Ambient Pressure on an Airblast Spray Injected into a Crossflow,'' AIAA Paper 98-3903.